

Article

A Hybrid Biological-Adsorption Approach for the Treatment of Contaminated Groundwater Using Immobilized Nanoclay-Algae Mixtures

Sara Mollamohammada ¹, Ashraf Aly Hassan ^{2,*}, Mohamed Dahab ³ and Sandeep Kumar ⁴

- ¹ Engineering Department, Carroll College, Helena, MT 59625, USA; smollamohammada@carroll.edu
² Civil and Environmental Engineering and the National Water Center, United Arab Emirates University, Al Ain P.O. Box 15551, Abu Dhabi, United Arab Emirates
³ Civil Engineering Department, University of Nebraska-Lincoln, Lincoln, NE 68588, USA; mdahab@unl.edu
⁴ Department of Bio and Nano Technology, Guru Jambheshwar University of Science and Technology, Hisar 125001, Haryana, India; ksandeep36@yahoo.com
* Correspondence: alyhassan@uae.ac.ae; Tel.: +971-(03)-713-5334; Fax: +971-(03)-713-4343

Abstract: Mixing the *Scenedesmus* species with nanoclay and immobilizing in sodium alginate was evaluated as a sustainable treatment method for removing nitrate, atrazine, and metals from groundwater. Gel beads containing the hybrid mixture removed 100% of 10 mg/L N nitrate and 98% of 100 µg/L atrazine from synthetic groundwater in three days. The optimal amount of nanoclay was found to be 0.30 mg per bead. The experimental data fit well into a Freundlich adsorption isotherm and followed pseudo first-order kinetics. When tested in actual groundwater, 91% of nitrate and 100% of Cr, Se, and V were eliminated in three days without need for any nutrients or carbon source. Immobilizing algal beads embedded with nanoclay is a natural, low-cost alternative for groundwater treatment. The gel beads can be reused for at least two cycles without a compromise in performance. They are water-insoluble, easy to harvest, and offer high removal efficiency.

Keywords: *Scenedesmus* species; biological treatment; adsorption; nitrate removal; atrazine removal; nanoclay



Citation: Mollamohammada, S.; Aly Hassan, A.; Dahab, M.; Kumar, S. A Hybrid Biological-Adsorption Approach for the Treatment of Contaminated Groundwater Using Immobilized Nanoclay-Algae Mixtures. *Water* **2021**, *13*, 633. <https://doi.org/10.3390/w13050633>

Academic Editors: James A. Smith and Caetano C. Dorea

Received: 13 January 2021
Accepted: 22 February 2021
Published: 27 February 2021

Publisher's Note: MDPI stays neutral with regard to jurisdictional claims in published maps and institutional affiliations.



Copyright: © 2021 by the authors. Licensee MDPI, Basel, Switzerland. This article is an open access article distributed under the terms and conditions of the Creative Commons Attribution (CC BY) license (<https://creativecommons.org/licenses/by/4.0/>).

1. Introduction

Groundwater in rural area is suffering from the overuse of nitrogen-based fertilizers and herbicides. Nitrogen is an essential nutrient for plants and is used in various forms to enhance plants' growth. Excess nitrogen in soil infiltrates into the groundwater commonly in the form of nitrate [1]. Herbicides are synthetic organic compounds (i.e., pesticides) used to control weeds, insects, and a variety of other agricultural purposes. Many herbicides are water-soluble and may dissolve in groundwater. Atrazine is one of the most commonly used triazine herbicides in the US and is utilized to control broadleaf weeds. It is a concern to the water supply because of its toxicity, relatively long half-life (60 to 100 days), and poor sorption by soil ($K_{oc} = \sim 100$). In most cases, the source of atrazine in groundwater is caused by leaching near the wellhead due to atrazine loading, cleanup activities, or back siphoning accidents during spraying operations [2].

The US Environmental Protection Agency (US EPA) has set a maximum contaminant level (MCL) of 10 mg/L for $\text{NO}_3\text{-N}$ and 3 ppb for atrazine [3]. The EPA's database shows many cases of atrazine detection at concentrations above the MCL in groundwater in Delaware, Illinois, Indiana, Iowa, Kansas, Michigan, Minnesota, Missouri, Nebraska, and New York [4].

Exposure to drinking water with a nitrate level above the MCL is a potential health risk. Methemoglobinemia, which is the result of nitrate reduction to nitrite in infants' digestive system, is reported to be common in infants fed formula using well water with

elevated nitrate contamination [5]. Additionally, strong evidence relating drinking nitrate-contaminated water and colorectal cancer, thyroid disease, and neural tube defects was documented [6]. Nitrosamine is formed in water contaminated with nitrate and atrazine. Nitrosamines have been reported to increase the risk of developing Non-Hodgkin Lymphoma [7].

A microalgal-based water treatment system is a sustainable solution to remove nitrate; however, these systems also have disadvantages, such as expensive biomass harvesting [8]. Immobilization of microalgae in polymeric matrices is an attractive alternative that facilitates biomass harvesting and makes the operation more flexible [9]. Algal immobilized gels can be manufactured using both synthetic (e.g., polyurethane, poly vinyl alcohol) and natural (alginate, carrageenan, agar, chitosan) polymers. A proper carrier must be porous enough to allow the diffusion of the molecules from the bulk solution to the cells. For the autotrophic living algal cells, the carrier must be transparent and allow light transmission [10].

Several studies have been performed to evaluate the capability of immobilized algal beads in removing nutrients from aqueous solutions. Immobilized *Chlorella vulgaris* and *Scenedesmus rubescens* removed more than 90% of phosphate, nitrate, and ammonium from secondary, synthetic wastewater within nine days [11]. In our previous work, the removal efficiency of nitrate was evaluated in groundwater using immobilized *Scenedesmus* sp. (*S. sp.*) beads. The immobilized beads were able to remove 90% of the nitrate from groundwater in two days [12]. The mechanism of nitrate uptake by algal beads involves the adsorption of nitrate onto the surface of the bead, penetration into the polymer, and finally sorption into the cells [13]. Hence, a faster adsorption process could lead to a faster nitrate assimilation by microalgae, which will increase the nitrate removal rate considerably.

Adding an adsorbent to the algal beads will accelerate this process especially if it is positively charged to attract the negatively charged nitrate ions. Previous studies have evaluated the capability of adsorbent beads in groundwater remediation. In one study, the calcium–alginate beads embedded with nano zero valent iron (NZVI), magnetite nanoparticles (MNP), and powdered activated carbon (PAC) were used for nitrate removal from groundwater. The results showed that each gram of NZVI can remove 4.3–9.6 mg $\text{NO}_3\text{-N}$ in 48 h [14]. In another study, calcium alginate beads entrapping a mixture of Fe(0) and nanosized magnetite (NMT) were able to remove up to 94.5% nitrate in 48 h at the bead dosage of 37.5 g L^{-1} [15].

As an abundant low-cost natural adsorbent, clays have been successfully used in removing nitrate, heavy metals, and endocrine-disrupting chemicals from water [16,17]. Clays are primarily made of particles with at least one dimension in the nanometer scale; therefore, they can be regarded as nanoclay [18]. The specific surface area of the nanoclay can reach a few hundred m^2/g due to their small size. Their high surface area combined with their nano-size dimension and peculiar charge are three most important factors behind their large tendency to take up ions and organic compounds from water [17,18]. Several studies explored the application of nanoclay as an adsorbent for nitrate and atrazine removal. Clay mineral originating from a dam in Morocco was optimized for the adsorption of nitrate. The highest nitrate removal of 71.89% was achieved at $\text{pH} = 5.1$ using 1 g/L of adsorbent [19]. Clay minerals modified by a cationic surfactant were used in batch mode for the adsorption of pesticides. The results showed an increase in the adsorption rate compared to untreated clays, however, the adsorption coefficient of atrazine was found to be very low [20]. In another study, high sorption values of atrazine (98% after 18 h) on dye-clay complexes were achieved; however, the concentration of adsorbent used was very high (50 g/L) [17].

In this study, a mixture of algae (*S. sp.*) and positively charged nanoclay particles, immobilized on alginate gel (hybrid biological adsorption system), are evaluated for the removal of nitrate and atrazine from synthetic and actual groundwater. Because of its high surface area, nanoclay accelerates the adsorption of nitrate and atrazine from the bulk solution and results in a faster removal rate. Batch and sequential batch growth

studies are conducted to evaluate the treatment efficiency. The nitrate uptake capacity of the hybrid system is quantified based on different uptake mechanisms of adsorption, biological assimilation, and extracellular enzyme activity resulting from toxicity.

2. Materials and Methods

2.1. Cultivation of Algae

A sample of the microalgae strain *S. sp.* was obtained from the Biochemistry Department at the University of Nebraska-Lincoln. The microalgae were cultivated in a sterilized Bold's Basal Medium (BBM) that contained the essential inorganic salts and vitamins necessary to grow algae: B^{3+} , Ca^{2+} , Cl^{-} , Co^{2+} , CU^{2+} , Fe^{3+} , K^{+} , Mg^{2+} , Mn^{2+} , Mo^{6+} , NH_4^{-} , Na^{+} , SO_4^{2-} , Zn^{2+} , PO_4^{3-} , NO_3^{-} , p-aminobenzoic acid, biotin, cyanocobalamin, folic acid, nicotinic acid, pantothenic acid, pyriodoxine hydrochloride, riboflavin, thiamin hydrochloride, and thioctic acid concentration, and kept at room temperature (20 °C). The light necessary for algal growth was provided by sunlight and artificial plant light. The intensity of light varied between 600 and 700 Lux. After about two weeks of cultivation, the microalgae were used for bead preparation.

2.2. Preparation of Nanoclay-Embedded Algal Beads and Experimental Conditions

To prepare the nanoclay-embedded alginate–algae beads, the cells of *S. sp.* were first harvested by centrifugation at 3500 rpm for 10 min. The supernatant was discarded, and the cells were resuspended in deionized (DI) water and mixed with a 2% sodium alginate solution and a sufficient amount of nanoclay. The nanoclay mineral used in the experiments was purchased from Sigma Aldrich (St. Louis, MO, USA) and used as is after dissolution and sonication. The nanoparticles were treated with 25–30% *w/w* trimethyl stearyl ammonium (TMSA), a cationic surfactant. All the growth medium nutrients except nitrate were added to the suspension. TMSA was added based on its increased adsorption capacity [21]

A syringe pump (Harvard Apparatus, model 55-3333) was used to drop the mixture of algae, alginate, and nanoclay into a 2% calcium chloride solution. The uniform beads (diameter: 2.35 mm) were formed upon dropping the mixture into the calcium chloride solution and were left overnight to harden. Algal cell migration from the immobilized beads to the bulk solution was quantified and found negligible. As a control sample, blank beads were manufactured without incorporating any algal cells. The bead preparation process was outlined in our previous work [12]. The experiments were performed using synthetic and actual groundwater samples. Synthetic groundwater was prepared using DI water mixed with a target concentration of nitrate and/or atrazine. Potassium nitrate (99.9%, Sigma Aldrich) and analytical standard atrazine (99.9%, Sigma Aldrich) were used to achieve concentrations of 10 mg/L NO_3-N and 0.1 mg/L atrazine, respectively. The actual groundwater sample was collected from a pump station in the city of Hastings, NE and stored at 4 °C in a refrigerator. Before being used in the experiments, the suspended solids in groundwater were removed by filtering through a Whatman syringe filter membrane with a 0.45 mm pore size.

All the experiments were carried out in 500 mL flasks at 20 °C. The flasks were autoclaved for 20 min at 121 °C in order to prevent any contamination. Each flask contained 400 mL of the aqueous solution. The ratio of the beads/solution was 12.5% in all the reactors. According to our previous work, *S. sp.* shows higher nitrate uptake in heterotrophic conditions [12]. Therefore, the experiments involving synthetic groundwater were performed in heterotrophic growth mode, maintaining 125 mg/L glucose at each reactor as an organic carbon source. The concentration of chemical oxygen demand (COD) was used as a surrogate of glucose availability. When actual groundwater was used, no additional chemicals were provided to the beads or to the bulk solution and the water was used as received. All experiments were performed in triplicate and each result presented here is the mean of three replicated studies.

2.3. Analytical Measurements

A UV-vis spectrophotometer (Nano-Drop 2000, Thermo Scientific, Waltham, MA, USA) was used to measure the concentration of NO₃-N in all reactors. A new method based on vacuum-assisted sorbent extraction (VASE) (5800, EnTech Instruments, Simi Valley, CA, USA) was used with gas chromatography-mass spectrometry (GC-MS, 5977B, Agilent Technologies, Santa Clara, CA, USA) to measure the concentration of atrazine in the solutions. A dissolved oxygen (DO) meter (5100, YSI, Yellow Springs, OH, USA) was used to measure the concentration of DO in each reactor. Conductivity and pH of the bulk solution were measured using a conductivity meter (HQ14D, Hach, Ames, IA, USA) and a pH meter (Orion 3-star, Thermo Scientific, Waltham, MA, USA). TNTplus vial tests (TNT820, Hach, Ames, IA, USA) were used to record the COD of the bulk solution. The zeta potential of the beads was determined using a zeta potential analyzer (ZetaPals, Brookhaven Instruments, Holtsville, NY, USA).

Scanning electron microscopy (SEM) was used to examine the morphological structure of the beads. SEM images were taken using a Nova Nano SEM (FEI, Hillsboro, OR), with the voltage ranging between 2 and 5 kV. The beads were air dried first and coated with a thin layer of gold before imaging. The analysis of metals in the groundwater was performed using inductively coupled plasma mass spectroscopy (ICP-MS) (7500 CX, Agilent Technologies, Santa Clara, CA, USA).

2.4. Viability and Growth Assessment

The microscopic images of the algal colonies were taken using a Ti-S inverted fluorescence microscope (Nikon, Melville, NY, USA). An assessment of the viability of the algal cells within the immobilization matrix was performed by isolating the live cells from the background using the color threshold function in ImageJ v 1.51 j8.

2.5. Kinetic Models and Adsorption Isotherms

Two kinetics models, pseudo-first order and pseudo-second order, were applied in order to understand the dynamics of nitrate adsorption on ADSORPTION beads. The pseudo-first-order equation is shown as

$$\frac{dq_t}{dt} = K_1(q_e - q_t) \quad (1)$$

where q_e and q_t are nitrate adsorbed per unit mass of nanoclay (mg/g) at equilibrium and at time t (day), respectively, and K_1 (L/day) is the rate constant of first-order adsorption.

The pseudo-second-order process is

$$\frac{dq_t}{dt} = K_2(q_e - q_t)^2 \quad (2)$$

where q_e and q_t are defined in the same way as in the first-order reaction and K_2 (g/day.mg) is the constant of the second-order adsorption.

The isotherm of adsorption on the ADSORPTION beads was evaluated using the Langmuir and Freundlich models. The Langmuir isotherm is based on the assumptions that adsorption only occurs at specific homogeneous sites within the nanoclay–alginate matrix and the adsorbent is saturated after one layer of nitrate molecules forms on the surface of it. The Freundlich isotherm describes the adsorption of multilayer surfaces [22]. The linearized form of the Langmuir and Freundlich isotherms can be seen in Equations (3) and (4), respectively.

$$\frac{C_e}{q_e} = \frac{1}{q_0 K_L} + \frac{C_e}{q_0} \quad (3)$$

$$\log q_e = \log K_f + \frac{1}{n} \log C_e \quad (4)$$

where q_e is the amount of nitrate adsorbed per gram of nanoclay (mg/g), C_e is the equilibrium solution concentration of nitrate (mg/L), q_0 (mg/g) is the maximum capacity of nitrate required to form a complete monolayer on the surface, and K_L represents the Langmuir constant. K_f is the Freundlich adsorption constant, related to the adsorption capacity of the adsorbent, and n is the Freundlich exponent, related to the surface heterogeneity. q_e was calculated by Equation (5):

$$q_e = \frac{(C_0 - C_e)}{m} \cdot V \quad (5)$$

where C_0 and C_e (mg/L) are the initial and equilibrium nitrate concentrations, respectively, V (L) is the volume of the solution, and m (g) is the mass of the nanoclay.

3. Results and Discussion

3.1. Adsorption Capacity of Nanoclay on Algae–Alginate Matrixes

To evaluate the impact of nanoclay on nitrate uptake rate by the algal beads, batch studies were performed using four different groups of alginate gel beads embedded with nanoclay + algae (HYBRID), nanoclay (ADSORPTION), algae (BIOLOGICAL), and none (CONTROL).

As shown in Table 1, the HYBRID beads had the highest nitrate removal rate. They were able to remove 100% of nitrate in three days. The BIOLOGICAL beads uptook 43% of nitrate in this time. At day 3, the removal of $\text{NO}_3\text{-N}$ in the ADSORPTION and CONTROL groups were 20% and 10%, respectively. An increase in concentration of DO and pH and a reduction in COD were indicators of photosynthesis and glucose uptake by algal cells, which was highest in the BIOLOGICAL beads. No photosynthesis occurred in ADSORPTION and CONTROL beads because they did not have any algal cells and the nitrate uptake occurred through adsorption on the surface of the immobilization matrix. This could explain why the concentration of DO and COD was almost stable in these two groups of beads.

Table 1. Percentage of nitrate present and change in concentration of COD (mg/L), DO (mg/L), and pH of the solution over time.

| Day | HYBRID: Algae + Nanoclay | | | | ADSORPTION: Nanoclay | | | | CONTROL: None | | | | BIOLOGICAL: Algae | | | |
|-----|--------------------------|--------|------|------|----------------------|--------|------|------|---------------|--------|------|------|-------------------|--------|------|------|
| | C/Co | COD | pH | DO | C/Co | COD | pH | DO | C/Co | COD | pH | DO | C/Co | COD | pH | DO |
| 0 | 1.00 ± 0.00 | 156.80 | 7.71 | 8.60 | 1.00 | 160.00 | 7.02 | 7.80 | 1.00 | 160.00 | 8.36 | 8.20 | 1.00 ± 0.00 | 172.80 | 6.34 | 8.80 |
| 1 | 0.95 ± 0.19 | - | 7.76 | 9.33 | 0.96 | - | 6.51 | 8.20 | 1.01 | - | 6.56 | 8.80 | 0.88 ± 0.03 | - | 6.98 | 9.20 |
| 2 | 0.15 ± 0.01 | 139.50 | 7.54 | 9.34 | 0.87 | 161.00 | 6.30 | 8.10 | 0.90 | 155.00 | 6.44 | 8.30 | 0.67 ± 0.04 | 115.20 | 7.15 | 9.40 |
| 3 | 0.00 ± 0.00 | - | 7.09 | 9.40 | 0.80 | - | 6.17 | 8.10 | 0.90 | - | 6.17 | 8.30 | 0.57 ± 0.08 | - | 7.22 | 9.50 |
| 5 | 0.00 ± 0.00 | 152.00 | 6.99 | 9.43 | 0.75 | 155.00 | 5.94 | 8.10 | 0.88 | 152.00 | 5.64 | 8.00 | 0.40 ± 0.11 | 115.80 | 7.60 | 9.90 |

It is evident that the nanoclay addition accelerated the nitrate uptake rate by the algal beads. The uptake occurred through the HYBRID mechanism of consecutive nitrate adsorption on the nanoclay surface, followed by the assimilation by algal cells, as a physicochemical process. The availability of nitrate in high density around algal cells increased the assimilation rate and freed the surface for further adsorption. As described in Section 2.2, the nanoclay used in these experiments was treated with a cationic surfactant. The positively charged nanoclay enhances the adsorption properties of the beads and increases their tendency to adsorb the negatively charged entities, which was nitrate in this case. Hence, the dual mechanism of adsorption and assimilation of nitrate is made more efficient than each mechanism individually.

The fit of the pseudo-first-order and pseudo-second-order models showed that the adsorption followed the pseudo-first-order model. The pseudo-first-order model had a higher correlation coefficient (0.910) compared to the second-order model (0.770). In addition, the calculated $q_{e,cal}$ from the first-order model agreed with the experimental value (Table 2).

Table 2. Kinetic parameters for the adsorption of nitrate on nanoclay-embedded alginate beads.

| $q_{e,exp} \left(\frac{mg}{g}\right)$ | First-Order Adsorption | | Second-Order Adsorption | |
|---------------------------------------|--------------------------------|---------------------------------------|---|---------------------------------------|
| | $K_1 \left(\frac{1}{d}\right)$ | $q_{e,cal} \left(\frac{mg}{g}\right)$ | $k_2 \left(\frac{mg \cdot d}{g}\right)$ | $q_{e,cal} \left(\frac{mg}{g}\right)$ |
| 1.025 | 1.580 | 1.644 | 0.023 | 2.267 |

3.2. Impact of Nanoclay Dosage on Nitrate Uptake by the Beads

Varying amounts of nanoclay were added to alginate/algae beads to determine the effect of the mass of nanoclay on nitrate removal rate. The range changed from 0.0030 to 0.60 mg per bead and the removal efficiency of nitrate increased from 9.2% to 98.6% with a hundredfold increase in nanoclay concentration. The beads containing 0.30 and 0.60 mg nanoclay both showed significant nitrate uptake (98.8% and 98.2%, respectively).

The process of nitrate uptake in immobilized algal beads appears to start with adsorption of nitrate on the surface of the bead, followed by penetration into alginate and sorption into cells [12,13]. Therefore, adsorption on alginate gel and nanoclay and nitrate assimilation by algae cells could be the three major processes involved in the nitrate uptake process. Figure 1 separates these three processes. The adsorption rate by alginate beads was calculated from the nitrate uptake by the CONTROL beads (Section 3.1). The adsorption rate by nanoclay and the assimilation rate by microalgae are calculated using Equations (6) and (7):

$$A_{s,t} = A_{h,t} - A_{n,t} \quad (6)$$

where $A_{s,t}$ is the amount of nitrate assimilated by microalgae and $A_{h,t}$ and $A_{n,t}$ are the quantity of nitrate uptaken by HYBRID and ADSORPTION beads, respectively, after t days of operation.

Adsorption by nanoclay is calculated using Equation (7):

$$A_{d,t} = A_{n,t} - A_{c,t} \quad (7)$$

where $A_{d,t}$ is the amount of nitrate adsorbed by nanoclay and $A_{c,t}$ is the quantity of nitrate uptaken by the CONTROL beads after t days of operation.

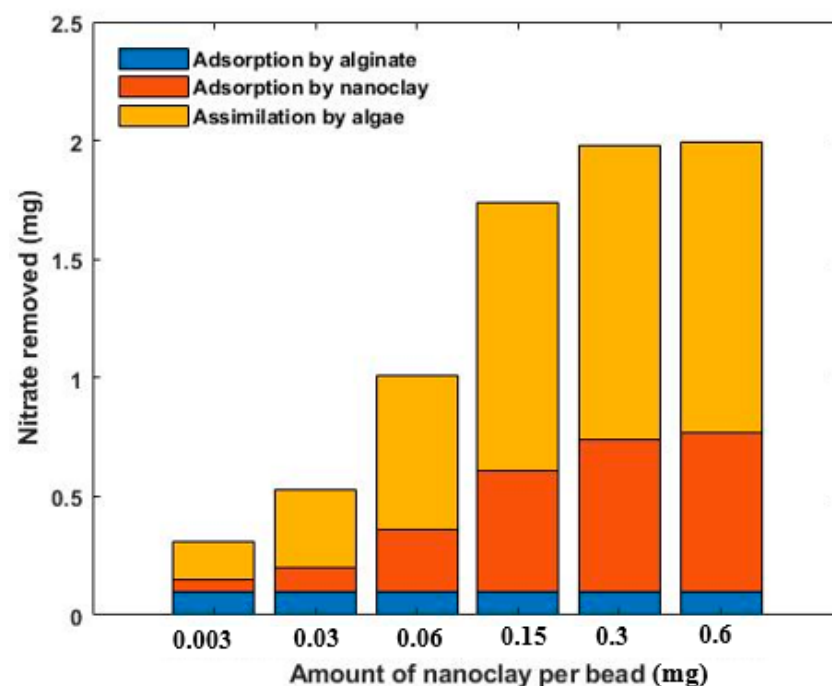


Figure 1. The mass of nitrate removed by the HYBRID beads embedded with different amounts of nanoclay after three days of operation. The initial concentration of nitrate was 10 mg NO₃-N/L.

Since the quantity of alginate was the same in all six groups of beads, the adsorption rate by alginate would be identical for all of them. According to Figure 1 the adsorption capacity of the nanoclay and assimilation rate by microalgae increased by increasing the dose up to 0.30 mg/bead and reached an equilibrium at this point. There was no significant change in the nitrate uptake rate at dosages higher than 0.30 mg/bead.

The zeta potential of the HYBRID beads was measured on different days of the operation. As shown in Table 3, increasing the nanoclay concentration increased the zeta potential of the beads at the beginning of the treatment process (day 0). The nanoclay used in these experiments was treated with TMSA, which contains a positive charge. Increasing the amount of nanoclay resulted in increased positive charge and consequently zeta potential. Throughout the treatment process, the zeta potential decreased and turned negative, confirming the accumulation of nitrate ions at the beads. The largest “negative” zeta potential coincided with the largest nitrate uptake at a concentration of 0.3 mg nanoclay/bead.

Table 3. Change in zeta potential of the HYBRID beads, embedded with different amount of nanoclay during 5 days of the treatment process.

| Day | Zeta Potential (mV) | | | | | CONTROL (No Nanoclay) |
|-----|---------------------|-------------------|------------------|--------------------|--------------------|--------------------------|
| | 0.003 mg | 0.03 mg | 0.15 mg | 0.30 mg | 0.60 mg | |
| 0 | -0.14 ± 0.021 | -1.14 ± -0.17 | 3.24 ± -1.2 | 3.46 ± 1.34 | 4.95 ± 0.12 | -1.42 ± -0.34 |
| 1 | -0.42 ± -0.024 | -1.35 ± -0.24 | -2.35 ± -1.1 | -5.2 ± -1.12 | -6.88 ± -2.41 | -2.89 ± 1.1 |
| 5 | -1.1 ± -0.21 | -5.2 ± -2.8 | -7.91 ± -2.5 | -11.71 ± -2.24 | -10.62 ± -1.44 | -4.5 ± -1.34 |

Increasing the nanoclay dose provided additional surface area and active sites available for the adsorption of nitrate. However, at levels larger than 0.30 mg/bead, the nanoclays aggregated, resulting in blockage of the active sites. Hence, no additional nitrate uptake was possible. Therefore, the concentration of 0.30 mg/bead was considered an optimum dose and was used in the experiments thereafter.

According to Figure 1, increasing the amount of nanoclay resulted in an assimilation rate increase by the microalgae. Accordingly, an increase in DO concentration was expected; however, this was not observed. Therefore, an additional fourth mechanism controlling the treatment by the HYBRID beads was proposed, involving the inherent toxicity of TMSA to the algal cells. TMSA causes some algal cells to break open. Accordingly, nitrate reductase (NR) enzymes were secreted outside of the cells. NR enzymes possess higher kinetic rates outside the cells since nitrate does not need to diffuse through the cell wall. This process facilitates the assimilation process. The accuracy of this theory is evaluated in Section 3.3.

The isotherm of adsorption on the ADSORPTION beads was assessed using the Langmuir and Freundlich models.

Nitrate adsorption data on the nanoclay alginate matrix fitted well to the Freundlich model and higher R^2 was derived in the Freundlich isotherm ($R^2 = 0.998$) than the Langmuir model ($R^2 = 0.912$). Using the Freundlich model, n and K_f were found to be 0.335 and 0.165, respectively.

In the Freundlich isotherm, the $1/n$ value describes the linearity of the adsorption process. The term $1/n = 1$ means that the reaction between solute and adsorbent is linear, whereas $1/n < 1$ indicates that the adsorption is unfavorable at lower equilibrium concentrations and the shape of the nonlinear adsorption isotherm is convex. The term $1/n > 1$ shows the concave shape of a nonlinear adsorption isotherm and means that the adsorption is more favorable at lower equilibrium concentrations [23]. The obtained value of $1/n$ equals 3.0, suggesting that adsorption of nitrate on a nanoclay–alginate matrix is more favorable at lower concentrations of nitrate.

3.3. The Role of TMSA in Nitrate Removal

TMSA is a widely used cationic surfactant. Due to its chemical stability and heat and pressure resistance, it is used as a raw material for producing hair conditioner, fabric softener, silicone oil, and rubber [24,25]. TMSA is reported to be toxic to *Chlorella* cells. Once inside the cell, TMSA may affect thylakoid organization and chlorophyll synthesis, which results in impairment of photosynthetic capacity and lowers the number of live cells. Although the mechanisms of TMSA toxicity may vary in different algae species, it is generally accepted that such toxicity impacts the structure of algal lipid membranes, binding with or denaturing membrane proteins. This causes increased membrane permeability and the leakage of compounds such as ions and amino acids that are significant for cell viability [26].

The toxicity of TMSA to algal cells might be the main reason behind the enhanced nitrate removal rate observed in the HYBRID beads (Section 3.2). With cells breaking open, NR enzymes are released and made more readily available for nitrate uptake. To check the accuracy of this theory, the algal cells were mixed with different quantities of TMSA, immobilized in alginate, and tested for nitrate uptake. The nanoclay that was used in this study contained ~30% (by wt.) TMSA. This means that the HYBRID beads with concentrations of 0.06, 0.15, and 0.30 mg nanoclay/bead contained 0.02, 0.04, and 0.09 mg TMSA, respectively. These ratios were used to make TMSA-embedded algal beads.

A live cell assessment was performed to check the toxicity of TMSA to the algal cells. Figure 2 compares the number of live cells in algal beads, embedded with 0.02, 0.04, and 0.09 mg TMSA over time. As shown, at day 0, the number of live cells was slightly higher in the cells embedded with a lower mass of TMSA. In all three groups, the number of live cells decreased over time.

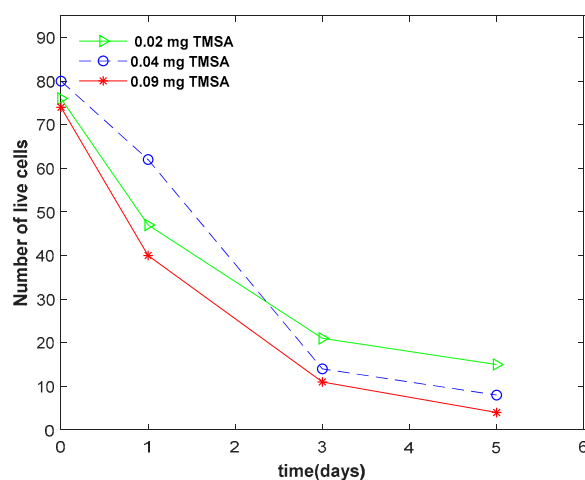


Figure 2. Change in the number of live cells in algal beads with 0.02 g, 0.04, and 0.09 mg TMSA per bead over time.

The amount of nitrate uptake by TMSA embedded beads was measured one day after the start of the experiments. As shown in Figure 3a, the beads containing 0.02, 0.04, and 0.09 mg TMSA removed 0.78 ± 0.144 , 0.69 ± 0.17 , and 0.65 ± 0.18 mg of nitrate, respectively. This was about twice as high as the removal observed by the HYBRID beads embedded with nanoclay possessing the same masses of TMSA. After three days of experiments, the removal rate reached its maximum, which was 3.27 ± 0.05 mg nitrate (Figure 3b).

In the TMSA-embedded beads, there was a direct contact between the algal cells and TMSA. Due to the inherent toxicity of TMSA to the algal cells, the main mechanism controlling the treatments here could be the death of the cells and releasing the NR enzymes to the bulk solution, which accelerates the nitrate removal rate.

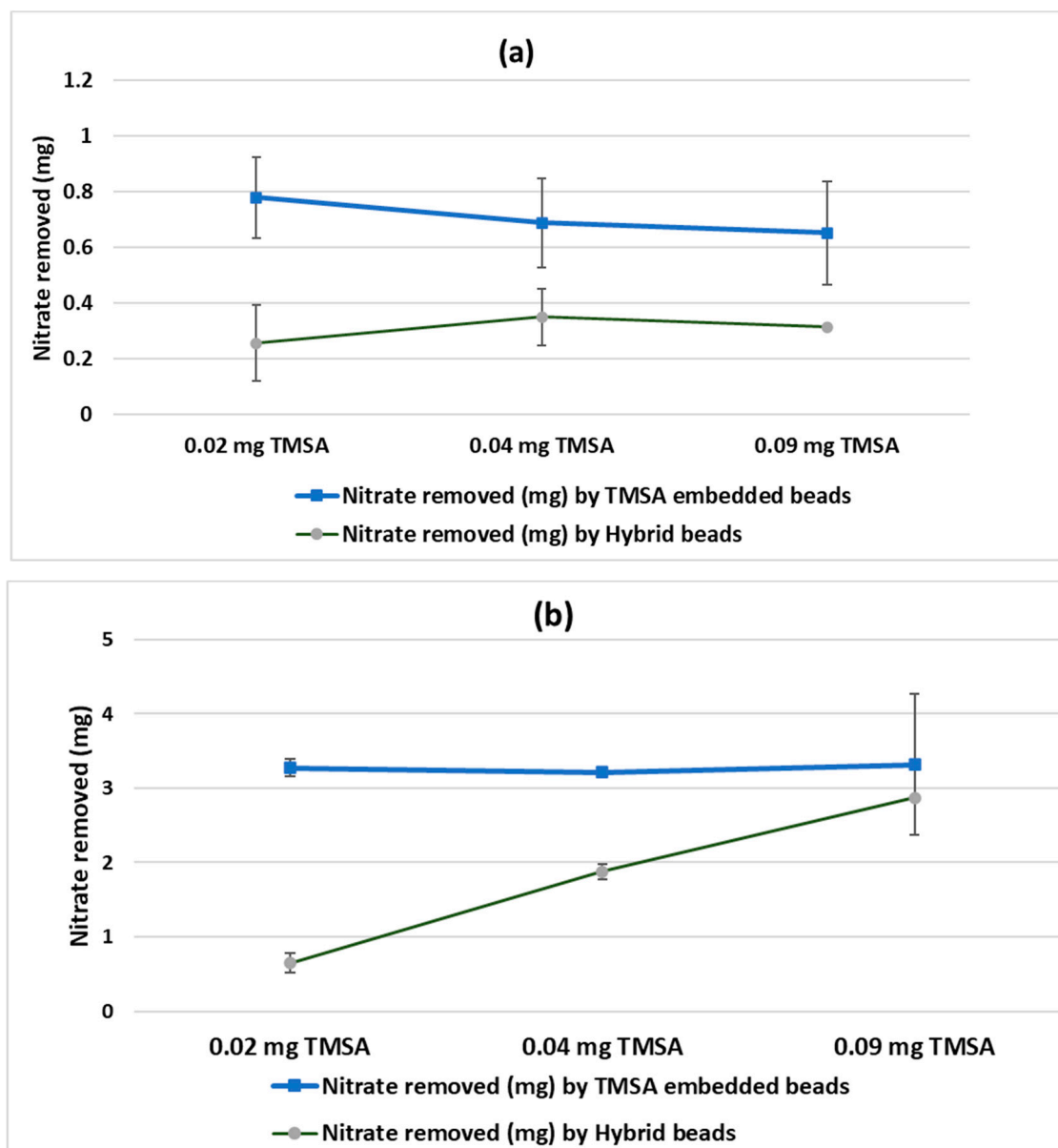


Figure 3. Mass of nitrate removed after (a) 1 day and (b) 3 days of operation as affected by the mass of TMSA and nanoclay embedded in the beads.

It is possible that the extracellular enzyme activity is the fourth mechanism controlling the treatment in the HYBRID beads, and the main reason behind the high nitrate uptake observed in Section 3.2.

3.4. Evaluation of the Performance of Nitrate Removal under Sequential Batch Conditions

Although nitrate was successfully removed in batch reactors, the durability of the treatment system was tested in sequential batch mode. The experiments were conducted in triplicate reactors for three consecutive treatment periods. At the end of each period, the treated water in each reactor was discarded and the reactors were filled back up with synthetic groundwater and glucose. Aside from the nutrients embedded within the beads during manufacturing, no additional nutrients were provided. As shown in Figure 4, the nitrate removal rate decreased from 96.2% to 47.5% over periods 1 to 3. Over time, the turbidity of the solution increased from 1.2 Nephelometric Turbidity Units (NTU) (day 1) to 10.6 NTU (day 25), which could be a sign of nanoclay leaching out of the beads and entering the groundwater matrix. In sequential batch mode, nutrients and calcium may

get washed out of the reactors by discarding the treated water at the end of each period. Calcium is an essential ion for the stability of the beads. When the beads form, calcium ions bind to the blocks of alginate chains and the strength of the alginate gel is largely dependent on the number of cross-links formed [27]. Since the beads were not replaced throughout, the algal cells faced calcium and nutrient deficiency. This led to the loss of bead strength, lower nitrate assimilation, and reduced performance. The beads can be used for additional cycles if the treated water is rich in nutrient and calcium, as is the case with actual groundwater.

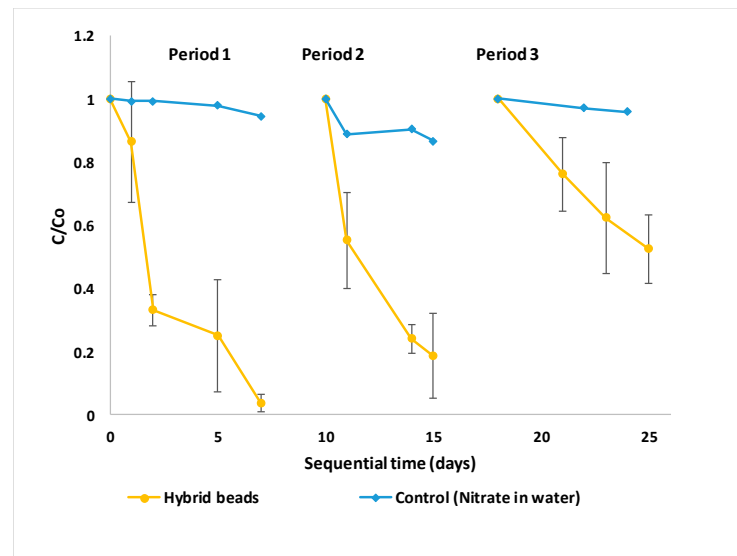


Figure 4. Nitrate present in the solution in sequencing batch mode.

3.5. Examination of the Efficiency of the Beads on the Removal Rate of Atrazine

Figure 5 displays the capability of the beads to remove atrazine from groundwater. Atrazine was reduced during the first 24 h of treatment by 86% using the HYBRID beads. The removal by the ADSORPTION beads was estimated at 64%. Therefore, the net percentage of atrazine removal by immobilized algal cells was 22%. On day 3, the removal efficiency reached the maximum of 98% for the HYBRID beads and 96% for the ADSORPTION beads. The removal rate for the ADSORPTION beads stayed constant until day 5, but it decreased to 85% for the HYBRID beads, which was a sign of atrazine migration from the beads back to groundwater. When tested with the BIOLOGICAL beads, 50% of the atrazine was removed after two days of operation. The removal rate decreased to 40% at day 5.

Clays modified using cations with large alkyl groups (e.g., TMSA) contain a paraffin-like layer of organic phase in the interlayer of the clay lattice [28]. This layer acts as the partition medium for the sorption of the organic compounds. Sorption of atrazine on TMSA-modified nanoclay was a function of the organic phase in the interlayer of nanoclay, following the adsorption of cationic surfactants (TMSA) in the lattice [29]. The mechanism of atrazine removal by algae was not previously reported, and it may involve biosorption, bioaccumulation, or biodegradation. Atrazine is considered toxic to many strains of green algae. However, the toxicity of the atrazine depends on the strain of algae and the exposure time. For *Scenedesmus*, the median effective concentration (EC_{50}) ranges between 21–49 ppb [30]. The initial concentration of atrazine used in these experiments was 100 ppb, which is higher than the inherent toxicity of atrazine to the algal cells. Therefore, after three days of exposure, the atrazine molecules slowly started to leave the cells and transfer to the bulk solution, which caused an 11% reduction in uptake rate for the HYBRID and BIOLOGICAL beads.

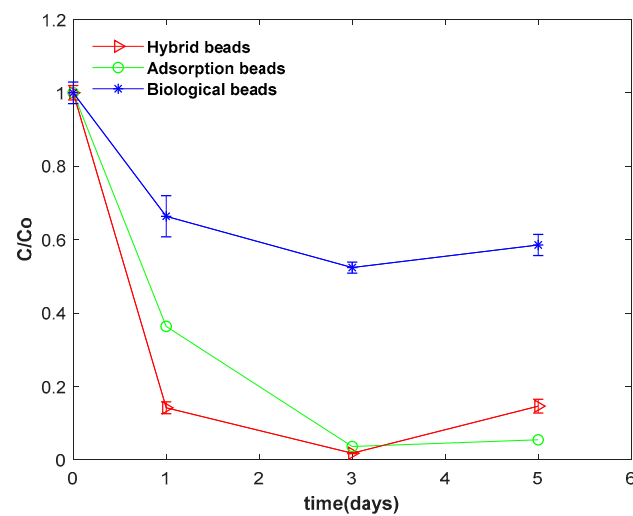


Figure 5. Percentage of atrazine present in the solution over time. The initial concentration of atrazine was 0.1 mg/L.

The solid/water distribution coefficient K_d was calculated to evaluate the effectiveness of the adsorption on alginate beads in uptaking nitrate and atrazine. K_d was calculated using the following equation:

$$K_d = \frac{c_i - c_e}{c_e} \times \frac{V}{m} \quad (8)$$

where C_i and C_e are the initial and final (equilibrium) concentrations of the contaminant in solution (mg/L), V is the volume of the solution (L), and m is the mass of the adsorbent (g) [31]. The distribution coefficients are shown in Table 4.

Table 4. Distribution coefficient (K_d) for nitrate and atrazine adsorption from groundwater.

| Matrix | K_d ($\frac{l}{g}$)—Nitrate Adsorption | K_d ($\frac{l}{g}$)—Atrazine Adsorption |
|--|--|---|
| ADSORPTION beads (nano clay + alginate) | 0.148 | 3.85 |
| CONTROL beads (alginate) | 0.109 | 0.231 |

The higher K_d represents more effectiveness of the adsorbent material in removing target contaminants from the aqueous solution. As shown in Table 4, adding nanoclay to the alginate beads increases the distribution coefficient from 0.231 to 3.85 L/g and improves the adsorption of atrazine significantly. There is also a slight increase in nitrate removal when alginate beads are mixed with nanoclay. However, the greatest performance in nitrate uptake occurs when nanoclay is added to the mixture of algae and alginate and the uptake occurs through the combined mechanisms of adsorption, biological assimilation, and extracellular enzyme activity, as discussed in Section 3.2.

3.6. Application of Actual Groundwater

The capability of the HYBRID beads to remove nitrate and metals from actual groundwater was tested. The raw groundwater was tested for the concentration of nitrate and metals prior to the experiments. A complete analysis of the groundwater is shown in Table 5.

Table 5. Analysis of the actual groundwater, collected from Hastings Utilities, Nebraska.

| Parameters | Concentration |
|-------------------|---------------|
| Nitrate (ppm) | 9.07 ± 1.04 |
| Sodium (ppm) | 49.30 ± 0.21 |
| Magnesium (ppm) | 21.34 ± 0.18 |
| Potassium (ppm) | 10.09 ± 0.04 |
| Calcium (ppm) | 120.45 ± 0.29 |
| Sulfur (ppm) | 26.18 ± 0.19 |
| Phosphorous (ppm) | 2.76 ± 0.006 |
| Zink (ppb) | 19.50 ± 0.18 |
| Chromium (ppb) | 1.06 ± 0.07 |
| Vanadium (ppb) | 2.83 ± 0.07 |
| Arsenic (ppt) | 1706 ± 36 |
| Molybdenum (ppt) | 1251 ± 106 |
| Lithium (ppt) | 24,882 ± 257 |
| Boron (ppt) | 61,544 ± 1248 |
| Manganese (ppt) | 11,873 ± 114 |
| Nickel (ppt) | 1393 ± 103 |
| Selenium (ppt) | 2299 ± 42 |

The HYBRID and BIOLOGICAL beads removed 91% and 93% of nitrate from groundwater within three days without requiring any external organic carbon source. Both autotrophic and heterotrophic mechanisms were active in the BIOLOGICAL beads and the photosynthesis was the driving force behind the pH increase. The removal rate remained constant for the BIOLOGICAL beads and in the HYBRID beads, it reached 99% after six days. The uptake of nitrate by ADSORPTION and CONTROL beads during this period was 35% and 12%, respectively (Table 6).

Table 6. Percentage of nitrate present in the solution, pH, and COD of the bulk solution over time in actual groundwater.

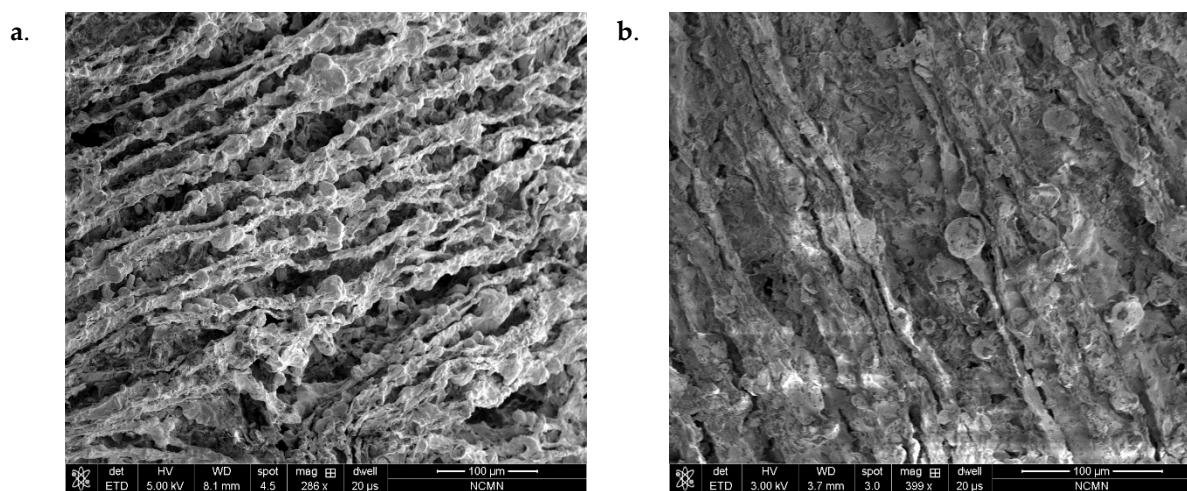
| Day | HYBRID: Algae + Nanoclay | | | ADSORPTION: Nanoclay | | | CONTROL: None | | | BIOLOGICAL: Algae | | |
|-----|--------------------------|--------|------|----------------------|--------|------|---------------|--------|------|-------------------|--------|-------|
| | C/Co | COD | pH | C/Co | COD | pH | C/Co | COD | pH | C/Co | COD | pH |
| 0 | 1.00 ± 0.00 | 166.33 | 7.31 | 1.00 ± 0.00 | 180.00 | 7.32 | 1.00 | 164.50 | 7.42 | 1.00 ± 0.00 | 172.00 | 7.30 |
| 1 | 0.89 ± 0.09 | 86.00 | 7.62 | 0.90 ± 0.03 | 90.00 | 7.64 | 0.94 | 162.00 | 7.25 | 0.40 ± 0.04 | 146.00 | 8.59 |
| 2 | 0.58 ± 0.07 | 138.00 | 8.42 | 0.76 ± 0.04 | 115.60 | 8.16 | 0.92 | 158.20 | 7.12 | 0.08 ± 0.03 | 133.00 | 8.18 |
| 3 | 0.09 ± 0.07 | 120.00 | 8.06 | 0.72 ± 0.08 | 121.00 | 8.37 | 0.93 | 160.00 | 7.68 | 0.07 ± 0.03 | 132.00 | 9.50 |
| 5 | 0.02 ± 0.03 | 194.80 | 7.74 | 0.69 ± 0.05 | 112.50 | 8.27 | 0.88 | 162.40 | 7.77 | 0.07 ± 0.02 | 124.60 | 10.03 |
| 6 | 0.01 ± 0.01 | 196.80 | 8.03 | 0.65 ± 0.09 | 123.20 | 8.10 | 0.88 | 160.00 | 7.93 | 0.07 ± 0.02 | 110.00 | 10.02 |

Some of the metals present in the groundwater were fully or partially removed by the HYBRID beads (Table 7). SEM analysis was performed to study the surface morphologies of the HYBRID beads before and after exposure to the groundwater. SEM images show that the fresh beads had a porous, heterogeneous surface. The pores and cavities on the beads facilitated the sorption of nitrate and metals (Figure 6a). After exposure to the groundwater the size of the pores decreased, and the beads became smoother and compact (Figure 6b).

The main process involved in the removal of metals by immobilized beads is biosorption, which is described as follows: The metal ions are first transferred from the solution to the biosorbent surface, which contains different functional groups that act as active binding sites [31,32]. The metal ions then diffuse into the pores of the adsorbent and eventually on the surface of the material [33]. In the HYBRID beads, the surface properties of the clay and the abundant functional groups of the gel provided adequate adsorption for the uptake of metals and facilitated the treatment process.

Table 7. Metal removal efficiency of the HYBRID beads in groundwater.

| Metal | Removal Efficiency (%) |
|-------|------------------------|
| Mg | 14.0 |
| P | 40.6 |
| S | 4.2 |
| V | 100.0 |
| Cr | 100.0 |
| Mn | 54.4 |
| Zn | 100.0 |
| As | 27.8 |
| Se | 100.0 |
| Fe | 72.0 |

**Figure 6.** SEM images of immobilized nanoclay-embedded *S. sp.* cells on the surface of sodium alginate at day 0 (a) and day 3 (b) of operation.

4. Conclusions

This study investigated the capability of nanoclay-embedded *S. sp.* beads to remove nitrate, atrazine, and metals from aqueous solutions. The experimental data show that embedding the algal beads with nanoclay accelerates the nitrate removal rate. From the studies conducted, it was established that a pseudo-first-order kinetic model described the kinetic rate of nanoclay-embedded alginate beads, and the equilibrium data fitted the Freundlich isotherm well.

Due to the inherent toxicity of atrazine to algal cells, the nanoclay-embedded alginate beads were found to be more effective in atrazine removal in the long run.

Nanoclay-embedded beads were proven to be a potential technique for the remediation of water contaminated with nitrate or atrazine owing to its exceptional uptake capacity as well as high selectivity for this anionic contaminant and herbicides. This target water is typically found in the ground- and surface water around farmlands. This technology is simple to establish and operate. It can be adapted by large farms as well as private households using contaminated well water. The system can also be used for the treatment of groundwater in surface ponds prior to recharge or at the point of use.

Author Contributions: Conceptualization, A.A.H.; methodology, A.A.H. and S.M.; formal analysis, A.A.H. and S.M.; investigation, S.M.; resources, A.A.H. and M.D.; data curation, S.M.; writing—original draft preparation, S.M.; writing—review and editing, A.A.H., M.D. and S.K.; visualization, A.A.H. and S.M.; supervision, A.A.H. and M.D.; project administration, A.A.H.; funding acquisition, A.A.H. All authors have read and agreed to the published version of the manuscript.

Funding: This work was supported by the University of Nebraska-Lincoln Research Council (Seed Grant), National Water Center, United Arab Emirates University (UAEU) (Grant Number G00003297), and HSCST, Govt. of Haryana, India (Grant No. HSCST/R&D/2018/2103. The authors gratefully acknowledge the technical support provided by ENTECH INSTRUMENTS and Hastings Utilities in performing this work.

Data Availability Statement: Not applicable.

Conflicts of Interest: The authors declare no conflict of interest.

References

1. Sebilio, M.; Mayer, B.; Nicolardot, B.; Pinay, G.; Mariotti, A. Long-term fate of nitrate fertilizer in agricultural soils. *Proc. Natl. Acad. Sci. USA* **2013**, *110*, 18185–18189. [[CrossRef](#)]
2. Isensee, A.R.; Helling, C.S.; Gish, T.J.; Kearney, P.C.; Coffman, C.B.; Zhuang, W. Groundwater residues of atrazine, alachlor, and cyanazine under no-tillage practices. *Chemosphere* **1988**, *17*, 165–174. [[CrossRef](#)]
3. U.S. Environmental Protection Agency. *Edition of the Drinking Water Standards and Health Advisories Tables*; U.S. Environmental Protection Agency: Washington, DC, USA, 2018.
4. U.S. Environmental Protection Agency. *National Primary Drinking Water Regulations*; U.S. Environmental Protection Agency: Washington, DC, USA, 1995.
5. Greer, F.R.; Shannon, M. Infant methemoglobinemia: The role of dietary nitrate in food and water. *Pediatrics* **2005**, *116*, 784–786. [[CrossRef](#)] [[PubMed](#)]
6. Ward, M.H.; Jones, R.R.; Brender, J.D.; De Kok, T.M.; Weyer, P.J.; Nolan, B.T.; Van Breda, S.G. Drinking water nitrate and human health: An updated review. *Int. J. Environ. Res. Public Health* **2018**, *15*, 1557. [[CrossRef](#)]
7. Rhoades, M.G.; Meza, J.L.; Beseler, C.L.; Shea, P.J.; Kahle, A.; Vose, J.M.; Spalding, R.F. Atrazine and nitrate in public drinking water supplies and non-Hodgkin lymphoma in Nebraska, USA. *Environ. Health Insights* **2013**, *7*, 15–27. [[CrossRef](#)] [[PubMed](#)]
8. Eroglu, E.; Agarwal, V.; Bradshaw, M.; Chen, X.; Smith, S.M.; Raston, C.L.; Iyer, K.S. Nitrate removal from liquid effluents using microalgae immobilized on chitosan nanofiber mats. *Green Chem.* **2012**, *14*, 2682–2685. [[CrossRef](#)]
9. Fierro, S.; del Pilar Sánchez-Saavedra, M.; Copalca, C. Nitrate and phosphate removal by chitosan immobilized *Scenedesmus*. *Bioresour. Technol.* **2008**, *99*, 1274–1279. [[CrossRef](#)]
10. Moreno-Garrido, I. Microalgae immobilization: Current techniques and uses. *Bioresour. Technol.* **2008**, *99*, 3949–3964. [[CrossRef](#)]
11. Garbisu, C.; Gil, J.M.; Bazin, M.J.; Hall, D.O.; Serra, J.L. Removal of nitrate from water by foam-immobilized *Phormidium laminosum* in batch and continuous-flow bioreactors. *J. Appl. Phycol.* **1991**, *3*, 221–234. [[CrossRef](#)]
12. Mollamohammada, S.; Hassan, A.A.; Dahab, M. Nitrate removal from groundwater using immobilized heterotrophic algae. *Water Air Soil Pollut.* **2020**, *231*, 1–13. [[CrossRef](#)]
13. Hameed, M.A. Effect of algal density in bead, bead size and bead concentrations on wastewater nutrient removal. *Afr. J. Biotechnol.* **2007**, *6*, 1185–1191.
14. Bahrami, F.; Yu, X.; Zou, Y.; Sun, Y.; Sun, G. Impregnated calcium-alginate beads as floating reactors for the remediation of nitrate-contaminated groundwater. *Chem. Eng. J.* **2020**, *382*, 122774. [[CrossRef](#)]
15. Cho, D.; Song, H.; Kim, B.; Schwartz, F.; Jeon, B. Reduction of nitrate in groundwater by Fe(0)/magnetite nanoparticles entrapped in ca-alginate beads. *Water Air Soil Pollut.* **2015**, *226*, 1–10. [[CrossRef](#)]
16. Rezvani, P.; Taghizadeh, M.M. On using clay and nanoclay ceramic granules in reducing lead, arsenic, nitrate, and turbidity from water. *Appl. Water Sci.* **2018**, *8*, 131. [[CrossRef](#)]
17. Srinivasan, R. Advances in application of natural clay and its composites in removal of biological, organic, and inorganic contaminants from drinking water. *Adv. Mater. Sci. Eng.* **2011**, *2011*, 1–17. [[CrossRef](#)]
18. Yuan, G.; Wu, L. Allophane nanoclay for the removal of phosphorus in water and wastewater. *Sci. Technol. Adv. Mater.* **2007**, *8*, 60–62. [[CrossRef](#)]
19. El Ouardi, M.; Qourzal, S.; Alahiane, S.; Assabane, A.; Douch, J. Effective removal of nitrates ions from aqueous solution using new clay as potential low-cost adsorbent. *J. Encapsulation Adsorption Sci.* **2015**, *5*, 178–190. [[CrossRef](#)]
20. Sanchez-Martin, M.; Rodriguez-Cruz, M.; Andrades, M.; Sanchez-Camazano, M. Efficiency of different clay minerals modified with a cationic surfactant in the adsorption of pesticides: Influence of clay type and pesticide hydrophobicity. *Appl. Clay Sci.* **2006**, *31*, 216–228. [[CrossRef](#)]
21. Siddiqi, R. Removal of Nitrates from Stormwater Using Nanoclays. Master's Thesis, California Polytechnic State University, San Luis Obispo, CA, USA, 2017.
22. Wu, X.; Hui, K.; Hui, K.S.; Lee, S.; Zhou, W.; Chen, R.; Son, Y. Adsorption of basic yellow 87 from aqueous solution onto two different mesoporous adsorbents. *Chem. Eng. J.* **2012**, *180*, 91–98. [[CrossRef](#)]
23. Mohsenipour, M.; Shahid, S.; Ebrahimi, K. Nitrate adsorption on clay kaolin: Batch tests. *J. Chem.* **2015**, *2015*, 1–7. [[CrossRef](#)]
24. Henton, D.E. Process for Coagulating a Grafted Rubber Compound. Patent WO/1990/013591, 1989.
25. Murray, A.M. Hair Conditioning Composition. Patent EP1282389A1, 2001.
26. Qv, X.Y.; Jiang, J.G. Toxicity evaluation of two typical surfactants to *Dunaliella bardawil*, an environmentally tolerant alga. *Environ. Toxicol. Chem.* **2013**, *32*, 426–433. [[CrossRef](#)]

27. Li, L.; Fang, Y.; Vreeker, R.; Appelqvist, I.; Mendes, E. Reexamining the egg-box model in calcium-alginate gels with X-ray diffraction. *Biomacromolecules* **2007**, *8*, 464–468. [[CrossRef](#)]
28. Boyd, S.A.; Jaynes, W.F.; Ross, B.S. Immobilization of organic contaminants by organo-clays; application to soil restoration and hazardous waste containment. In *Organic Substances and Sediments in Water*; Baker, R.A., Ed.; Lewis Publishers: New York, NY, USA, 1989; p. 199.
29. Dutta, A.; Singh, N. Surfactant-modified bentonite clays: Preparation, characterization, and atrazine removal. *Environ. Sci. Pollut. Res.* **2015**, *22*, 3876–3885. [[CrossRef](#)] [[PubMed](#)]
30. Larsen, D.P.; Stay, F.; Shiroyama, T.; DeNoyelles, F., Jr. Comparisons of single-species, microcosm and experimental pond responses to atrazine exposure. *Environ. Toxicol. Chem. Int. J.* **1986**, *5*, 179–190. [[CrossRef](#)]
31. Hamoudi, S.; Belkacemi, K. Adsorption of nitrate and phosphate ions from aqueous solutions using organically- functionalized silica materials: Kinetic modeling. *Fuel* **2013**, *110*, 107–113. [[CrossRef](#)]
32. Petrovič, A.; Simonič, M. Removal of heavy metal ions from drinking water by alginate-immobilized *Chlorella sorokiniana*. *Int. J. Environ. Sci. Technol.* **2016**, *13*, 1761–1780. [[CrossRef](#)]
33. Maznah, W.W.; Al-Fawwaz, A.; Surif, M. Biosorption of copper and zinc by immobilized and free algal biomass, and the effects of metal biosorption on the growth and cellular structure of *Chlorella* sp. and *Chlamydomonas* sp. isolated from rivers in Penang, Malaysia. *J. Environ. Sci.* **2012**, *24*, 1386–1393. [[CrossRef](#)]